

Cooling an array of multiple heat sources by a row of slot air jets

A.S. Huzayyin, S.A. Nada, M.A. Rady, A. Faris *

Mechanical Engineering Department, Benha High Institute of Technology, Benha 13512, Egypt

Received 6 December 2004; received in revised form 7 September 2005

Available online 9 March 2006

Abstract

An experimental study of cooling an array of multiple heat sources simulating electronic equipment by a single row of slot air jets positioned above a critical row (row having maximum heat dissipation rate) of the array was conducted. The other low power rows of the array were cooled by the spent air flow from the air jets. The experimental work was carried out in two phases. In the first phase, each block of the array was heated at a time and the other blocks of the array were kept unheated. The Nusselt number of each heated block and the thermal wake effect on downstream blocks were investigated and correlated for different values of jet Reynolds number, position of the block with respect to the jet impingement point and the separation distance between the orifice plate and the impingement surface. A superposition technique was implemented to demonstrate the practical importance of the present correlations in predicting the operating temperature of any block in an array with multiple heated blocks. In the second phase, the experiments were carried out with heating all the blocks at the same time. This phase was carried out to verify the superposition technique used to predict the operating temperature of the blocks of the array in the case of the multiple heating.

© 2006 Elsevier Ltd. All rights reserved.

Keywords: Jet cooling; Multiple heat sources; Slot jets; Thermal wake; Wake function

1. Introduction

Cooling of electronic equipment becomes nowadays an essential safety parameter in the field of electronics industry. The development of any electronic packaging is related to the availability of efficient cooling techniques that are capable of removing the expected high rates of heat dissipation. Air cooling is the most widely used cooling techniques in low power electronic systems for its simplicity in design, maintenance and its low installation and operating costs. In a typical electronic package with air cooling, heat dissipating elements are mounted in a circuit board, which is stacked within an enclosure. Cooling is accomplished using a fan or a blower to move the air with a low velocity through the passages of the enclosure. Many investigators simulated this cooling process of electronic equipment by an array of rectangular blocks placed on the bottom plate

of two parallel plates with the cooling air flowing through the passages between the plates. This arrangement of cooling is called in-line array parallel flow cooling. Many experimental and theoretical investigations to predict the operating temperature of the blocks, which is the most important factor in the design of the electronic equipment, under different geometrical and operating conditions were carried out. Moffat and his group [1–6] had extensively experimentally studied various aspects of thermal-hydraulic behavior of the arrays of the electronic equipment cooled by air flow through the passages of the array. The overall objective of their effort had been to develop the techniques of using the heat transfer coefficient and the superposition approach for predicting the temperature distribution in a regular array of cubical elements simulating electronic equipment under different geometrical and operating conditions. Sparrow et al. [7,8] studied heat transfer and pressure drop in arrays in rectangular blocks with barriers and missing blocks. Wirtz and Dykshoorn [9] and more recently Molki et al. [10] conducted

* Corresponding author. Tel.: +20 026981475; fax: +20 0133230297.
E-mail address: amirfaris@yahoo.com (A. Faris).

Nomenclature

A	exposed surface area of the block, m^2	q_{conv}	heat dissipated from the block by convection, W
B	thickness of the blocks, m	q_{rad}	heat losses from the block by radiation, W
H	clearance distance between the jet orifice and the blocks, m	Re	air Reynolds number, dimensionless
h	heat transfer coefficient, $W/m^2 K$	S	pitch between each two adjacent blocks, m
I	electric current input to the block, A	T_b	back temperature of the block, $^{\circ}C$
k_a	thermal conductivity of air, $W/m K$	T_{enc}	enclosure wall temperature, $^{\circ}C$
k_b	thermal conductivity of the block material, $W/m K$	T_{in}	air inlet temperature, $^{\circ}C$
L	length of the block, m	T_s	average surface temperature of the block, $^{\circ}C$
M	factor defined by Eq. (11) or (14), dimensionless	V	applied voltage to the block, V
N	number of the block, dimensionless	X	dimensionless distance of a block from the jet point, dimensionless
Nu	Nusselt number, dimensionless	ε	emissivity of the block surface, dimensionless
Nu_0	Nusselt number at stagnation, dimensionless	σ	Stefan–Boltzman constant, $W/m^2 K^4$
q_{cond}	heat losses from the block by conduction, W	θ	thermal wake function defined by Eq. (4), dimensionless

experimental investigations to study heat transfer in the entrance region of an array of rectangular heated blocks. The focus of their works was on heat transfer coefficient and associated thermal wake effect. Jubran et al. [11] conducted an experimental investigation to explore the effect of the size of modules, the presence of cylindrical module, and the missing of a module on heat transfer coefficient and pressure drop of an array of rectangular modules for different Reynolds numbers.

More recently, Yang and Fu [12] carried out an experimental investigation for the thermal wake measurements in electronic modules in the presence of heat transfer enhancement devices. The enhancement devices were consisted of various sizes and shapes of ribs. Morris and Garimella [13,14] developed empirical correlations applicable for forced convection heat transfer from in-line arrays of three-dimensional heated elements in channels. Also, the temperature distribution within the thermal wake downstream of a three-dimensional obstacles was investigated. Recktenwald [15] examined the general problem of heat transfer from several electronic components. The use of the method of superposition and the heat transfer coefficient to predict the temperature of the components were discussed and introduced. Also, Azar and Moffat [4] conducted a series of experiments to study the effects of power value and power distribution from array of modules simulating electronic chips on different methods of calculating convection heat transfer coefficient. Results showed that heat transfer coefficients based on inlet and mean temperature of air have large variation with power variation, while heat transfer coefficient based on the temperature of the block when it was unheated is independent of the power distribution. This makes it attractive for calculating the temperature distribution in boards.

This type of in-line array parallel flow direct air cooling is suitable only for low to moderate heat dissipation rates. On

the other hand, convective cooling of high heat flux surfaces through single or multiple jet impingements is becoming increasingly common in the field of electronic equipment cooling where high rates of heat transfer are required. Although many previous investigations [16–27] were carried out in the field of jet impingement cooling to study the hydrodynamics and heat transfer of a heated surface by a jet for different working conditions, geometrical conditions, arrangements and system parameters, a very little work was performed for cooling an array of heated block by jet impingement. Wadsworth and Mudawar [28] performed an experimental study to investigate heat transfer from simulated chips by dielectric liquid slot jet. The chips were arranged in an array 3×3 and each has its own power and cooling slot jet. The experiments examined the effect of slot width, height of the confinement, and the liquid Reynolds number on convection heat transfer coefficient. Also, Hollworth and Durbin [29] carried out an experimental work to determine the performance of low velocity air jets used to cool multiple heat sources simulating electronic packages. A uniform array of modules, each was cooled by four round air jets in semi-confined arrangement was considered. Pressure drop, heat transfer characteristics, and the thermal wake have been studied.

Actually, most of the electronic equipment has several components mounted on one or more printed circuit boards. These components usually have different amounts of power dissipation and not all active at the same time. Only a single or a few critical components might have high power dissipation rates. It may then be practical to focus the impinging jet on these critical components and cooling the other less critical ones by the spent flow. System designer should search for information to calculate the expected component operating temperature due to self heating and wake effect. However such information is not available in the previous jet impingement studies.

In the present study experimental investigations of cooling an array of multiple protruding heat sources by a single row of slot air jets positioned above a critical row of the array were conducted. The parameters describing the geometry of the present array are representative for the range expected in electronic equipment. Experiments were carried out for different values of Reynolds number ($Re = 500\text{--}2500$) and jet-plate separation distance ($H/B = 2\text{--}8$). During a single experiment, one single block of the array was powered at a time and the other ones were kept not powered. Measurements of the blocks surface temperature at different locations are used to calculate the heated block Nusselt number and the thermal wake effect on downstream blocks. Useful design correlations were then proposed to be employed along with superposition technique to predict the operating temperature of any block in an array with multiple heated blocks. Experiments were also carried out with heating all the blocks at the same time to verify the validity and estimate accuracy of the proposed correlations.

2. Experimental facility and procedure

2.1. Experimental setup

A schematic diagram of the experimental setup is shown in Fig. 1. Air was supplied from a compressor through an air storage tank, then dried and filtered upstream of the test section. The flow rate was controlled by a pressure regulator and a hand-operated globe valve, and measured with an orifice flow meter with a digital manometer across the orifice. The orifice flow meter was calibrated using a laminar flow element with an accuracy of $\pm 2\%$. The air enters a jet plenum through a perforated air supply pipe, and then passes through a honeycomb to obtain a uniform air flow

at the entrance of the jet orifice. The jet plenum was a 17-mm thick wooden airtight box with outside dimensions $115 \times 90 \times 45$ cm. The front face of the box contains Plexiglas window for visual observations. The uniform air flow exiting from the honeycomb passes through the slot opened in an orifice plate. The orifice plate was 5-mm thick Plexiglas having five slot openings in one column positioned just above the middle column (the column that contains the critical blocks) of the array. Each slot opening has dimensions of 5 mm width and 50 mm length. The geometric center of each slot was aligned with the geometric center of the corresponding block. The array of the heated blocks contained 45 modules, simulating multiple electronic modules, arranged in 5 rows and each row contains 9 elements. The pitch (S) between each two blocks was 68 mm. The blocks array was mounted on a movable Plexiglas plate which represents the bottom of the jet plenum box. This plate moves up and down using four screws spindles to change the clearance distance H between the orifice plate and the heated blocks. The blocks of the array were 50 mm \times 50 mm square blocks having a thickness $B = 6.5$ mm and made of bakelite, which is considered as a thermal and electric insulation. Only the nine blocks of the middle row of the array are active heated modules and all the other blocks of the array are dummy modules. These nine active heated blocks were covered from above with an electric wired board that produces the required input power. The heated block in the middle of this row (row number 3 and column no 5) is simulated as the only critical heated module under the jet. This block represents the critical module having a maximum power in this row. This block is denoted by M_0 and the other four blocks on the left and on the right of this block are denoted by $M_1, M_2, M_3,$ and M_4 as shown in Fig. 1. The active blocks were heated by connecting them to a direct current electric power supply. The input voltage

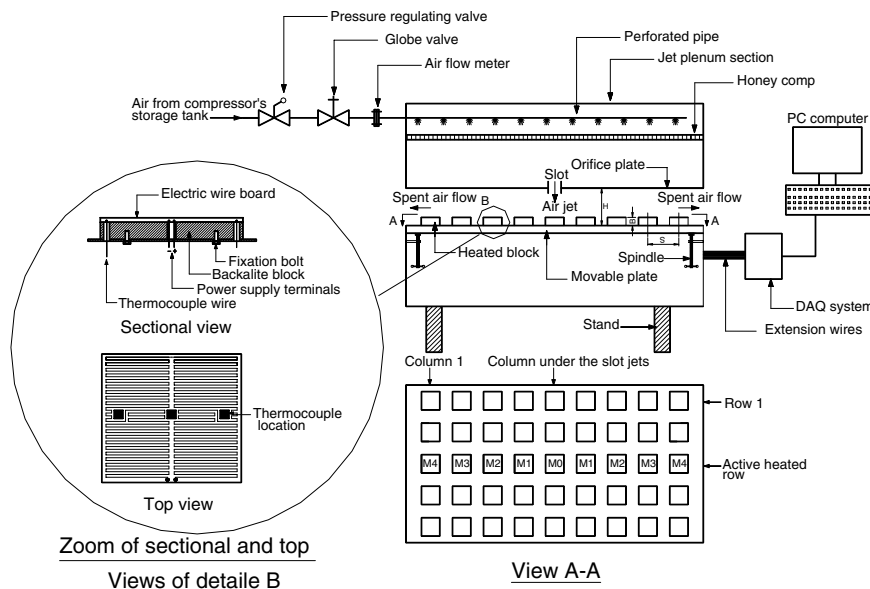


Fig. 1. Schematic diagram of the experimental setup.

and current to the heated block were controlled by the fine tunings of the power supply to keep the input power density constant at 0.2 W/cm^2 through all the experiments. Three type K-thermocouples junctions were fixed on each active heated block at equal space as shown in Fig. 1. To account the conduction heat losses from each block, another K-type thermocouple was fixed on the back of each active heated block. Also to account the radiation heat losses a thermocouple was fixed on the side wall of the jet plenum box. The readings of these thermocouples were recorded by a personal computer through a data acquisition system. The air passes through the slots of the orifices plate, hits the middle column of the blocks array and the spent air discharged from both sides of this column passes over the modules of the other columns.

2.2. Experimental conditions

The ranges of the test variables used in this study were:

Power density for each block	0.2 W/cm^2
Air Reynolds number (Re) based on the hydraulic diameter of the slot and properties of inlet air	500–2500
Dimensionless clearance distance (H/B)	2–8

2.3. Experimental procedure and program

The procedure and experimental program were as follows:

1. Adjust the clearance distance H/B between the jet orifice plate and the plate carrying the blocks array to the required value.
2. Supply and adjust power to the block M_0 of the active row.
3. Open the air flow and adjust the required Reynolds number and allow air jet to flow over the blocks surface.
4. Wait until steady state condition is achieved.
5. Record all instruments readings (voltage, current, pressure and temperature).
6. Repeat steps 3–5 for different Reynolds numbers (500, 1000, 1500, 2000, and 2500).
7. Repeat steps 3–6 with each of the blocks M_1 , M_2 , M_3 , and M_4 powered at a time.
8. Repeat steps 3–6 with all the blocks powered at the same time.
9. Repeat steps 2–7 for different values of H/B .

2.4. Data reduction

2.4.1. Nusselt number

In order to calculate the heat transfer coefficient at a certain block, the experiment was carried out with this block being the only heated block and the other blocks of the array were kept unpowered [1–6,15]. Power density input

to the block, inlet air temperature T_{in} (which was taken as the reference temperature to calculate to calculate the heat transfer coefficient) and average surface temperature of the heated block T_s (average of the readings of the three thermocouples fixed on the block) were required. The variation of the readings of the three thermocouples fixed on the block surface was within 2°C . The heat transfer coefficient for the block number i when it was the only heated block of the active row was calculated from

$$h_i = \frac{q_{\text{conv},i}}{A(T_{s,i} - T_{in})} \quad (1)$$

where A is the exposed surface area of the block and $q_{\text{conv},i}$ is the convection heat dissipated from the block. The convection heat transfer from the block was obtained by subtracting the conduction and the radiation heat losses from the heat input to the block. A simple one-dimensional conduction analysis of the heated block and an assumption of that the block is completely surrounded by an enclosure which was considered as a black body at a uniform temperature which equal to the side walls temperature of the enclosure, were used to calculate these losses. Therefore the heat dissipated by convection from the block can be expressed as

$$\begin{aligned} q_{\text{conv},i} &= VI - (q_{\text{cond}} + q_{\text{rad}}) \\ &= VI - \left(k_b A \frac{T_{s,i} - T_b}{B} + \varepsilon \sigma A [T_{s,i}^4 - T_{\text{enc}}^4] \right) \end{aligned} \quad (2)$$

where V and I are the electric current and the voltage input to the block, T_b is the back temperature of the block, B is the thickness of the block, k_b is its thermal conductivity and equal 0.23 W/mK for Bakelite, ε is its emittance and equal 0.15 for copper sheet (see Suryanarayana [30]) and T_{enc} is the temperature of the enclosure side walls which was very close to the surrounding temperature. The conduction and the radiation heat losses for the experiments were within 7% and 3% , respectively. The Nusselt number of the block i based on its length (L) is calculated from

$$Nu_i = \frac{h_i L}{k_a} \quad (3)$$

where k_a is the air thermal conductivity calculated at T_{in} . The Nusselt number of the heated block (M_0) placed at the impingement point of the air jet is called the stagnation Nusselt number and denoted by Nu_0 .

2.4.2. Thermal wake function

The heat dissipated by convection from a heated block raises the temperatures of the downstream unheated blocks. The contribution of heat output from a heated block to the temperature rise of the downstream unheated blocks is known by thermal wake and expressed in dimensionless form by what is called thermal wake function [1–6,15] as follows

$$\theta_{(i,j)} = \frac{T_{\text{un},(i,j)} - T_{in}}{T_{s,i} - T_{in}} \quad (4)$$

where $\theta_{(i,j)}$ is the thermal wake function of the unheated block i due to the power output from the upstream heated block j , $(T_{un(i,j)} - T_{in})$ is the temperature rise of the unheated block i due to the power output from the heated block j and $(T_{s,j} - T_{in})$ is the temperature rise of the heated block j due to its self heating.

2.4.3. Superposition technique

In the case of heating multiple blocks at the same time, the superposition technique [1–6,15] can be used to predict the temperature rise of a certain block from the experiments of heating each block of the array at a time as follows

$$T_{m,i} - T_{in} = (T_{s,i} - T_{in}) + \sum_{j=1}^{j=i-1} (T_{un(i,j)} - T_{in}) \tag{5}$$

(Temperature rise of block i in the case of multiple heated blocks) (Temperature rise of block i when it was heated alone)

(Temperature rise of block i due to upstream heated blocks)

Substituting by Eqs. (1)–(4) in Eq. (5), one can get

$$T_{m,i} - T_{in} = \frac{L_i q_{conv,i}}{A_i k_a Nu_i} + \sum_{j=1}^{j=i-1} \frac{L_j q_{conv,j}}{A_j k_a Nu_j} \theta_{(i,j)} \tag{6}$$

Correlating Nu and θ from the single heated block experiments in terms of the system parameter, the last equation

can be used to estimate the temperature rise of a block in the array in the case of multiple heated blocks.

2.5. Experimental uncertainties

The quantities measured directly included the air flow rate, air temperature, block surface temperature, input voltage and current, and the geometric dimensions. The uncertainty in the various variables used in the determination of the Nusselt number and thermal wake functions were: 2% for the air flow rate, 0.25% for the electric current I , 0.25 for the voltage V , 0.2 °C for any temperature measurement, 0.0001 m for any distance measurements, 0.5% for the thermal conductivity of air, 2% for thermal conductivity of block material, and 5% for the emittance of the board. Following the procedure of Holman and Gajda [31], the uncertainties of the air Reynolds number, the adiabatic Nusselt number, and the thermal wake function were 2.5%, 5%, and 30%, respectively.

3. Results

3.1. Temperature rise

Fig. 2 shows the temperature rise of the blocks of the active row for different Reynolds numbers and at different clearance distances (H/B) in the case of heating the block

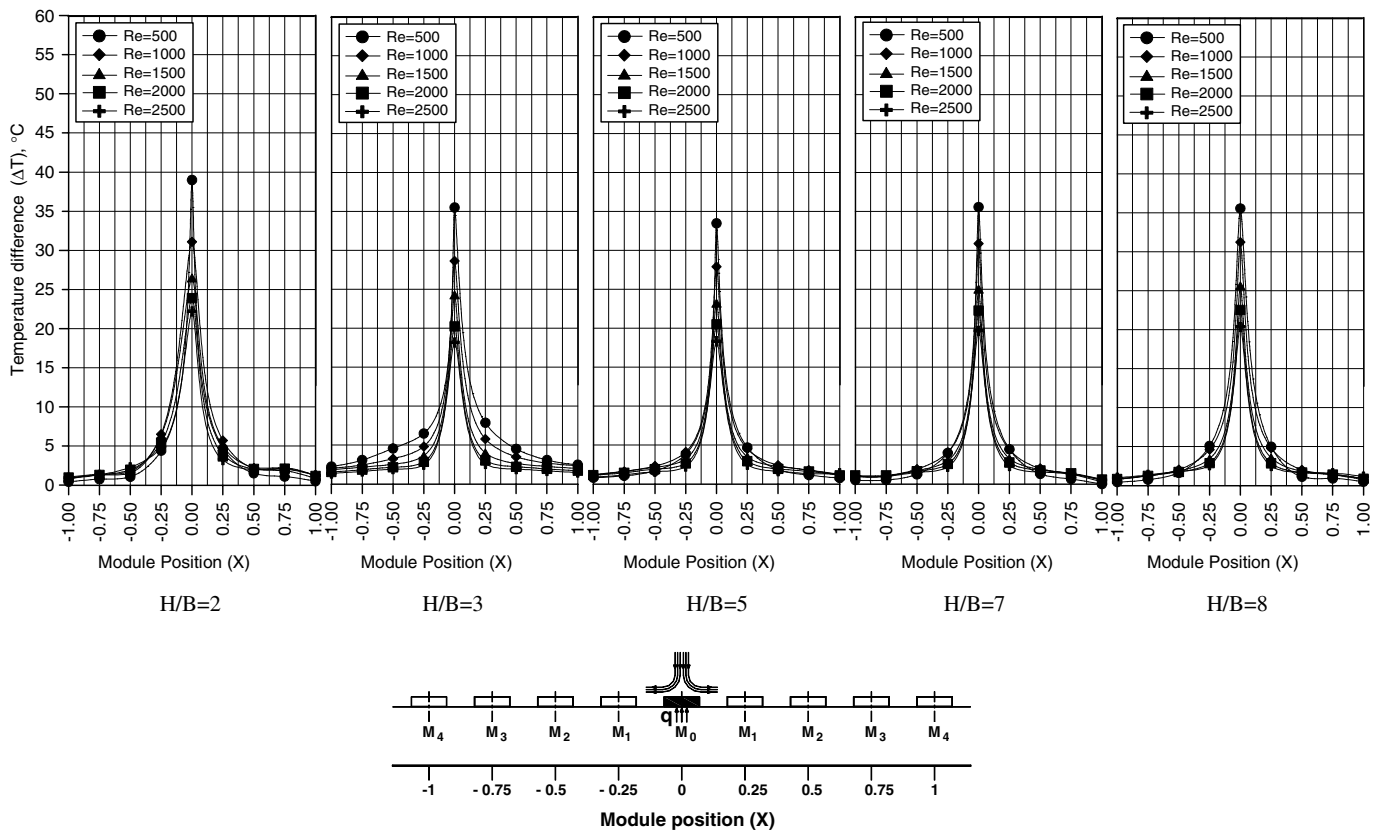


Fig. 2. Temperature rise of the blocks in the case of heating the block M_0 alone.

M_0 alone and keeping the other blocks M_1 , M_2 , M_3 and M_4 without heating. The coordinate of the figure X is a dimensionless distance which is the ratio between the distances of a block to that of M_4 measured from the jet impingement point, i.e. the position of M_0 , M_1 , M_2 , M_3 and M_4 are corresponding to $X = 0, 0.25, 0.5, 0.75$, and 1.0 , respectively. Fig. 2 shows the decrease of the temperature rise of the heated block M_0 with the increase of the air Reynolds number. This can be attributed to the increase of the heat removal rate from the block with the increase of the air Reynolds number. A careful examination of the numerical values of the different data points of Fig. 2 shows that the temperature rise of the heated block M_0 depends on the clearance distance (H/B); it decreases with the increase of H/B until a certain H/B beyond which the temperature rise increases with increasing H/B . The temperature rise was observed to be minimum at $H/B = 5$. This trend of the temperature rise agrees well with the previous study [24].

Also, Fig. 2 shows that the unpowered blocks M_1 , M_2 , M_3 and M_4 experience a temperature rise due to the thermal wake of the heated block M_0 . The temperature rise of these blocks comes from the heat gain from the spent air flow which was already heated during its impingement with the powered block M_0 . As the spent air flow passes on these blocks its temperature decreases and this explain the decrease of the temperature rise of these blocks in the direction of the spent air flow.

Fig. 3 shows the temperature rise of the blocks M_0 , M_1 , M_2 , M_3 and M_4 for different Reynolds number and at $H/B = 5$ in the case of heating each one at a time and keeping the others unheated. The figure shows that the temperature rise of the heated block increases as its X increases until $X = 0.25$ beyond which the temperature of the block remains approximately constant. This can be attributed to the hydrodynamics of the jet which shows a decelerating spent flow in the wall jet region until a fully developed was

obtained at approximately $X = 0.25$. The same trend of this figure was obtained for different values of H/B (see Faris [32]).

Fig. 4 shows the temperature rise of the blocks in the case of heating all the blocks at the same time for different Re at $H/B = 5$. Other curves for different H/B are given in Faris [32]. A careful comparison of the numerical values of this figure with those of Fig. 3 shows that the temperature rise of a certain block in the case of multiple heating of the blocks (Fig. 4) is higher than that if it was heated alone (Fig. 3). This can be attributed to the thermal wake effect

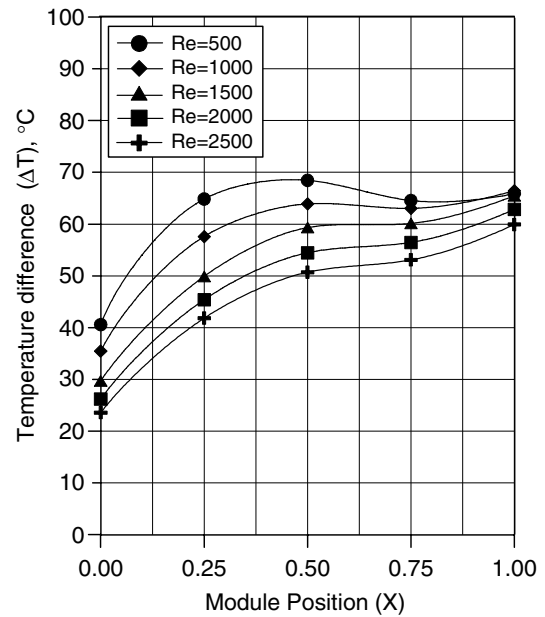


Fig. 4. Temperature rise of the blocks in the case of multiple heating ($H/B = 5$).

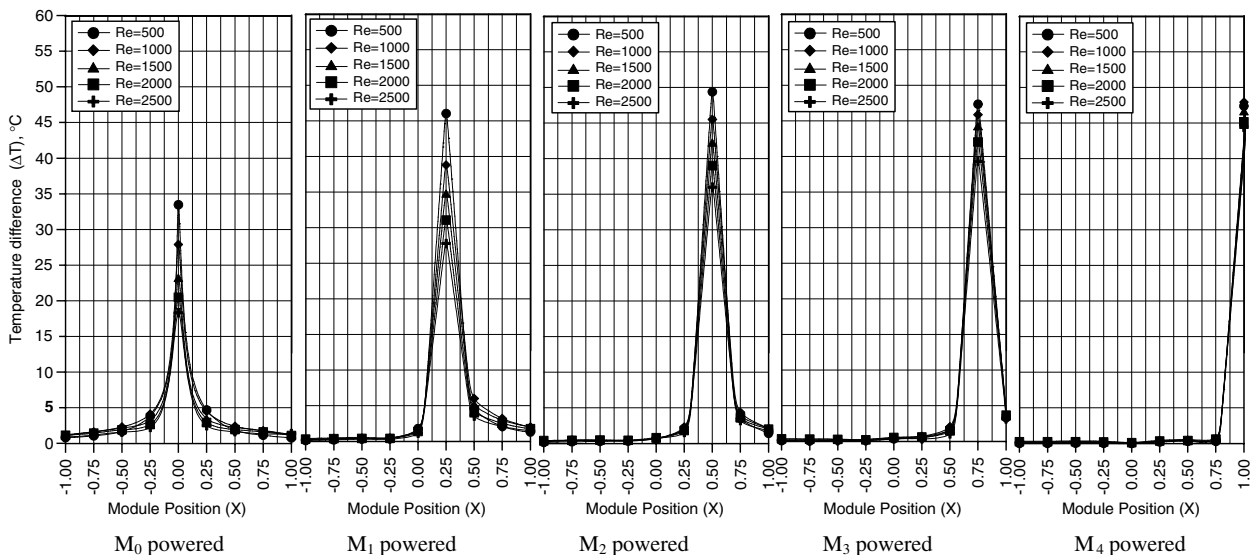


Fig. 3. Temperature rise of the different blocks in the case of powering each one at a time ($H/B = 5$).

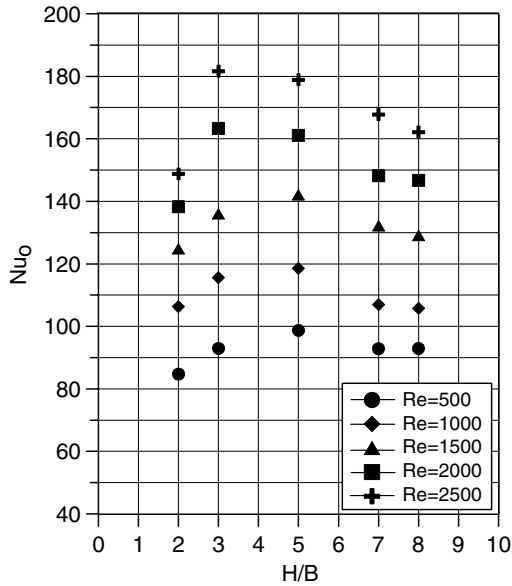


Fig. 5. Variation of stagnation Nusselt number with H/B and Re .

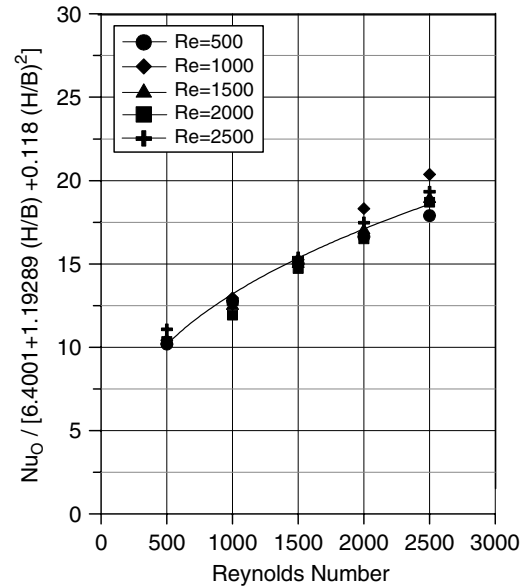


Fig. 6. Prediction using Eq. (7).

of each block on the other blocks in the case of multiple heating.

3.2. Stagnation Nusselt number

Fig. 5 shows the variation of the stagnation Nusselt number of the block M_0 situated under the slot air jet with the clearance distances H/B for different Air Reynolds numbers. As shown in the figure, for low Reynolds numbers ($Re \leq 1500$) the stagnation Nusselt number was

maximum at $H/B = 5$ and at high Reynolds numbers ($Re > 1500$) it was maximum at $H/B = 3$. This trend of the stagnation Nusselt number agrees well with the previous studies [24] which showed that the stagnation Nusselt number was maximum at a certain H . The clearance distance at which the maximum stagnation Nusselt number occurred was dependent on the Reynolds number and the orifice geometry and dimensions. Also Fig. 5 shows the increase of the stagnation Nusselt number with Re . This can be attributed to the decrease of the temperature

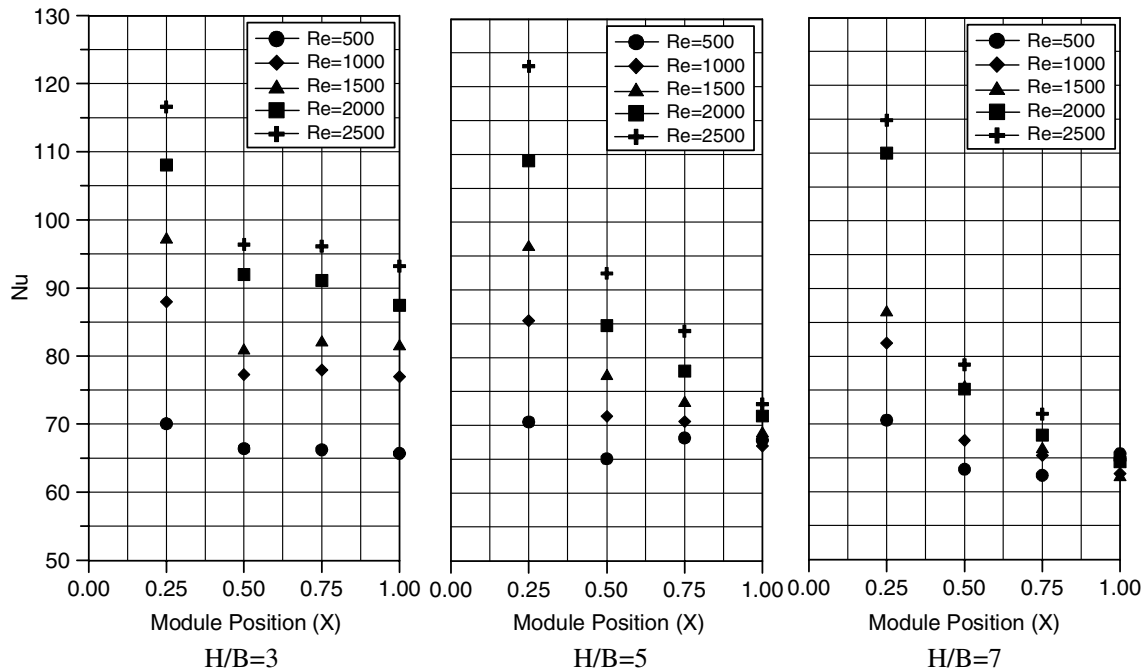


Fig. 7. Variation of Nusselt number with block position.

rise of the block with the increase of Re . This variation was expected and agrees well with the previous studies [16–27].

The variation of the stagnation Nusselt number with both Re and H/B can be correlated by the equations

$$Nu_0 = \{6.4001 + 1.1928(H/B) - 0.118(H/B)^2\}Re^{0.374} \quad (7)$$

The predictions of Nu_0 values using this correlation and the deviations of the data points are shown in Fig. 6. As shown in the figure, the correlation can predict the stagnation Nusselt number within $\pm 8\%$.

3.3. Nusselt number of the blocks $M_1, M_2, M_3,$ and M_4

The Nusselt numbers of the blocks $M_1, M_2, M_3,$ and M_4 , which were away from jet impingement point, are presented in Fig. 7 for different Re and H/B in the case of heating each one alone at a time. As shown in the figure, for all Re and H/B , the Nusselt number decreases as the distance of the block from the jet increases. The gradient of the Nusselt number decrease with increasing X . The decrease of the Nusselt number with increasing X can be attributed to the hydrodynamics of the jet which shows a decelerating spent air flow in the wall jet region. Also Fig. 7 shows the increase of the Nusselt number with the increase of Re and the decrease of H/B . This can be attributed to the increase of the spent flow velocity with the increase of Re and the decrease of H/B which leads to high heat removal rate and in consequence high Nusselt number. This trend of the Nusselt number agrees well with the previous studies [1–6] for cooling of in-line array blocks by parallel flows which showed the increase of the heat transfer coefficient of a block with both of the decrease of its distance from the entrance, the increase of air Reynolds number and the decrease of the channel height.

The variation of the Nusselt number of a block away from the jet can be correlated in terms X, Re and H/B as follows

$$Nu = 25.63X^{-0.1896}Re^{0.1783}(H/B)^{-0.1731} \quad (8)$$

The predicted values of Nu using this correlation and the deviations of the data points are shown in Fig. 8. As shown in the figure the correlation can predict the Nusselt number within $\pm 15\%$.

Eqs. (7) and (8) is valid only for slot width = 5 mm. It was possible, however, to use these equations with other correlations of previous works which relates the Nusselt number with slot width to predict the Nusselt numbers of the proposed cooling technique under different slot widths.

3.4. Thermal wake function

The present experimental results showed that the thermal wake effect of a heated block on the other downstream blocks depends on whether this heated block is directly under the jet or away from the jet.

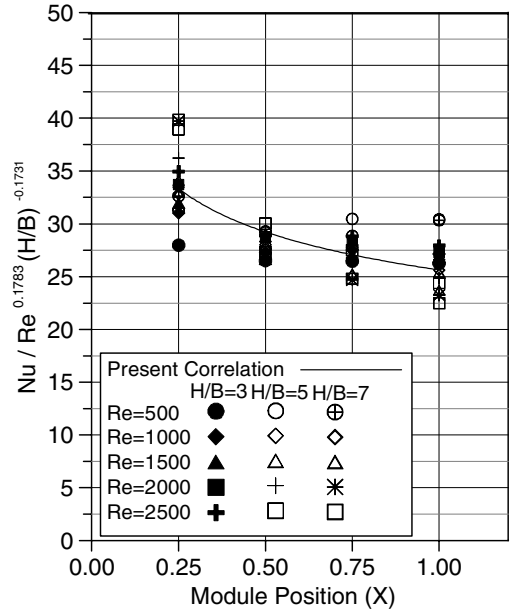


Fig. 8. Prediction using Eq. (8).

3.4.1. Thermal wake effect of a block under the jet (M_0)

The thermal wake function $\theta_{(1,0)}$ of the first unheated block situated immediately aside the heated block M_0 is presented in Fig. 9 as a function of Re with H/B as a parameter. The figure shows the decrease of $\theta_{(1,0)}$ with the increase of both of Re and H/B . The decrease of $\theta_{(1,0)}$ with the increase of Re can be attributed to the decrease of the spent flow air temperature with the increase of Re . The decrease of the spent flow air temperature leads to the decrease of the temperature rise of the downstream blocks. The decrease of $\theta_{(1,0)}$ with the increase of H/B can be attributed to the decrease of the velocity of the spent

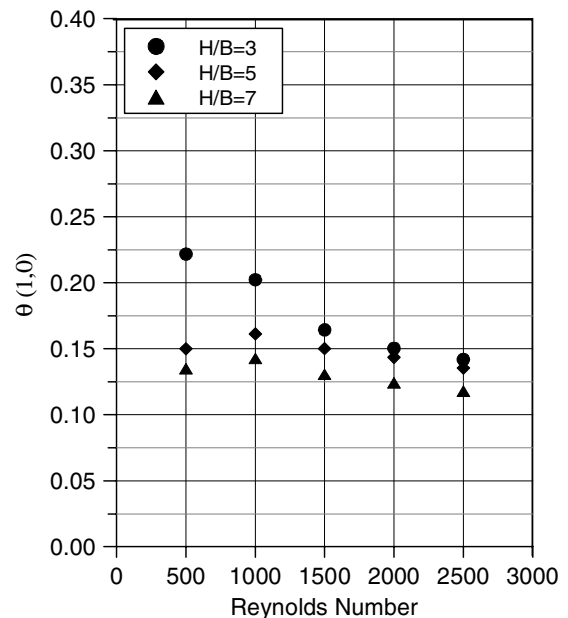


Fig. 9. Variation of $\theta_{(1,0)}$ with Re and H/B as a parameter.

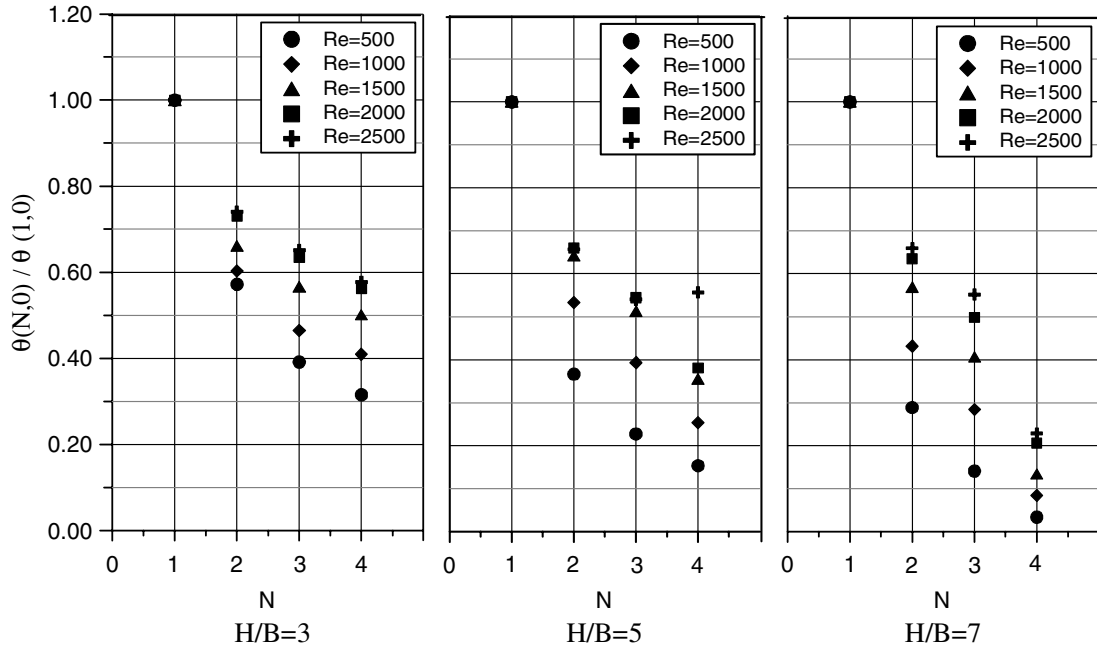


Fig. 10. Variation of $\theta_{(N,0)}/\theta_{(1,0)}$ with N taking Re and H/B as parameters.

flow with the increase of H/B which leads to low heat transfer rate from the spent air to the downstream blocks. The thermal wake function $\theta_{(1,0)}$ was correlated in terms of Re and H/B as follows

$$\theta_{(1,0)} = 0.738Re^{-0.149}(H/B)^{-0.34} \quad (9)$$

The thermal wake functions $\theta_{(N,0)}$, with $N = 2, 3$, and 4 , of the next downstream blocks M_2, M_3 and M_4 aside the heated block M_1 are presented in Fig. 10 as a function of N with Re and H/B as parameters. As shown in the figure, $\theta_{(N,0)}/\theta_{(1,0)}$ decreases with increasing N and increases with increasing Re and decreasing H/B . There are a number of

investigators who have correlated the data of cooling in-line array blocks by parallel flows as $\theta_{(N,0)}/\theta_{(1,0)} = 1/N$ (see Arvizu and Moffat [3] and Moffat et al. [5]) or as $\theta_{(N,0)}/\theta_{(1,0)} = (1/N)^m$ where m is a function of Re (see Wirtz and Dykshoom [9]). In this study the data is correlated as

$$\theta_{(N,0)}/\theta_{(1,0)} = (1/N)^m \quad (10)$$

with

$$m = Re^{-0.572}\{2(H/B)^2 - 9.73(H/B) + 44.37\} \quad (11)$$

The predictions of Eqs. (9) and (10) and the deviation of the data points from those predictions are shown in

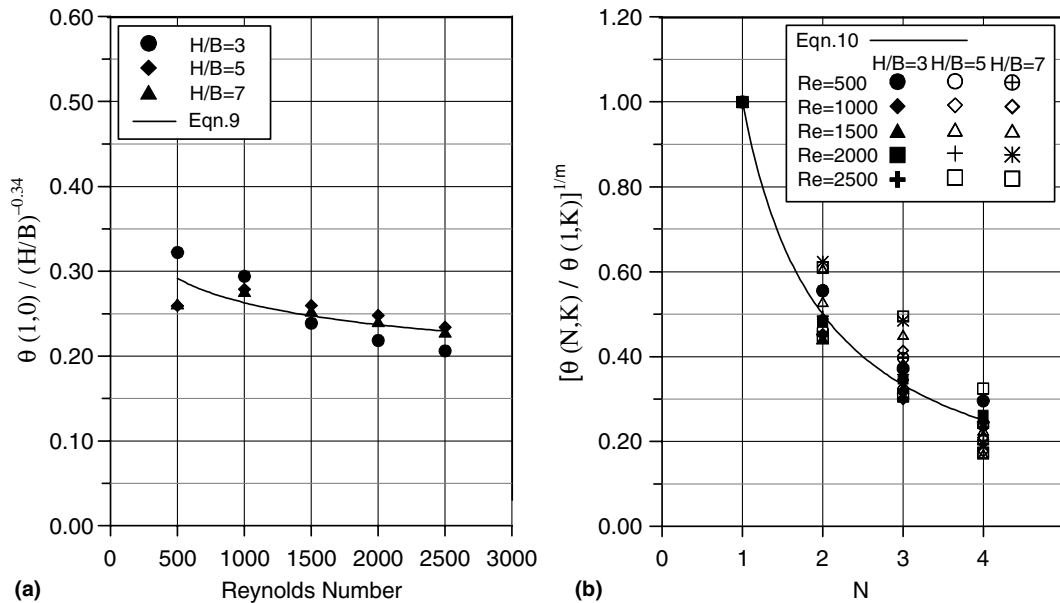


Fig. 11. Prediction of the thermal wake function due to M_0 heating. (a) Prediction of Eq. (9) and (b) prediction of Eq. (10).

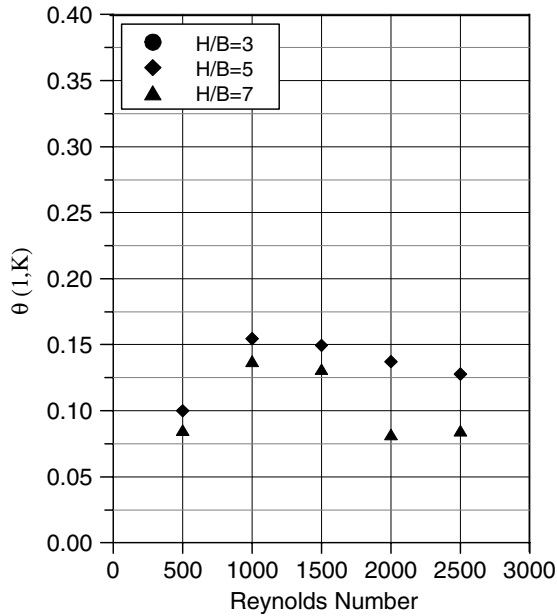


Fig. 12. Variation of $\theta_{(1,k)}$ with Re and H/B as a parameter.

Fig. 11. The correlations can predict $\theta_{(1,0)}$ and $\theta_{(N,0)}/\theta_{(1,0)}$ within $\pm 10\%$ and $\pm 30\%$, respectively. This deviation is within the uncertainty of measuring the wake function.

3.4.2. Thermal wake effect of a heated block away from the jet

In the case of heating any of the blocks away from the jet $M_1, M_2,$ or $M_3,$ the results of the present work, like those of Kim and Lee [33], showed that the location of the heated block does not have a marked effect on the wake function of the downstream blocks. Therefore, M_1 as the

heated block and the wake effect of this block on the downstream blocks $M_2, M_3,$ and M_4 is considered in this work.

The thermal wake function $\theta_{(1,k)}$ of the first unheated block situated immediately aside the k th-heated block, which is away from the jet, is presented in Fig. 12 as a function of Re with H/B as a parameter. It is evident from the figure that $\theta_{(1,k)}$ is slightly dependent on Re and decreases with the increase of H/B . This trend agrees with the results of Arvizu and Moffat [3] and Molki et al. [10] who showed that $\theta_{(1,k)}$ very slightly decreases with increasing Re in the case of cooling of in-line array by parallel flow. Also the present trend of $\theta_{(1,k)}$ is consistent with the results obtained by Wirtz and Dykshoorn [9] for cooling of in-line array in conventional channel flow, where an increase in channel wall to wall spacing reduced the thermal wake effect. The thermal wake function of the present work $\theta_{(1,k)}$ can be correlated in terms of H/B as follows

$$\theta_{(1,k)} = 0.56(H/B)^{-0.881} \tag{12}$$

The thermal wake function $\theta_{(N,k)}, N \geq 2,$ where N denoting the number of the block downstream the k -heated block, is presented in Fig. 13 as a function of N with Re and H/B as parameters. Also, the data can be correlated by

$$\theta_{(N,k)}/\theta_{(1,k)} = (1/N)^m \tag{13}$$

with

$$m = Re^{-0.284} \{2(H/B)^2 - 5.28(H/B) + 14.37\} \tag{14}$$

The predictions of Eqs. (12) and (13) and the deviation of the data points from those predictions are shown in Fig. 14. The correlations can predict $\theta_{(1,k)}$ and $\theta_{(N,k)}/\theta_{(1,k)}$ within $\pm 25\%$ and $\pm 35\%$, respectively. The deviation is close to the uncertainty of measuring the wake function.

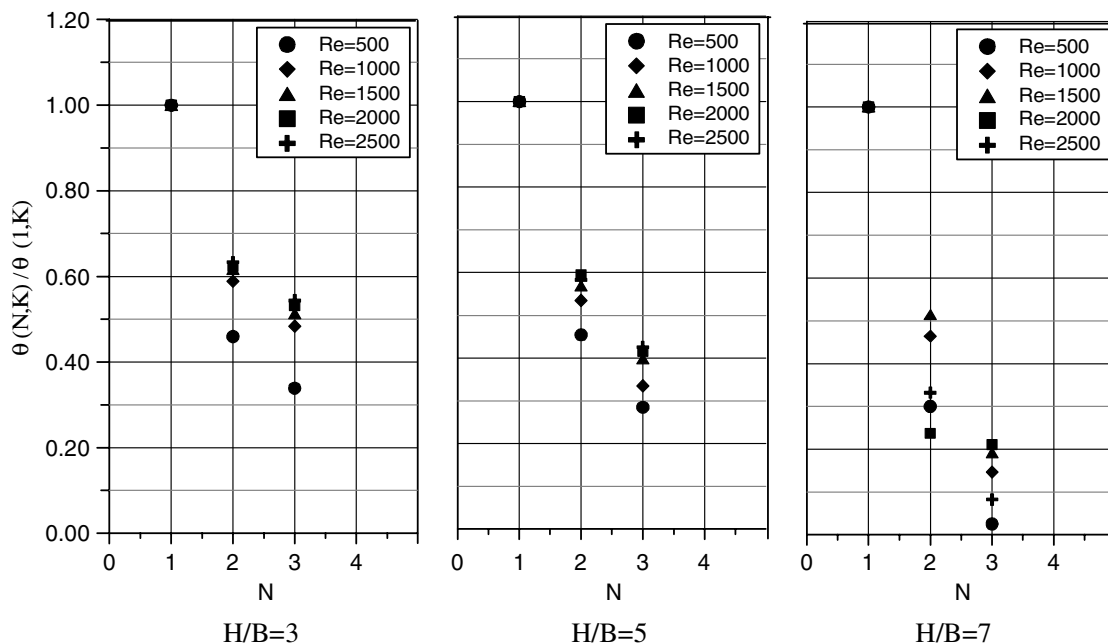


Fig. 13. Variation of $\theta_{(N,k)}/\theta_{(1,k)}$ with N taking Re and H/B as parameters.

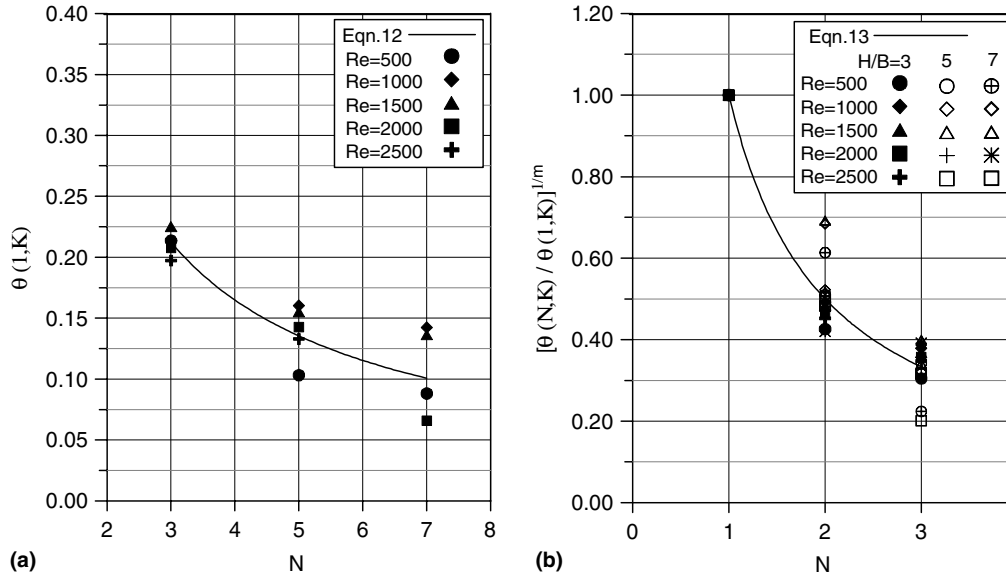


Fig. 14. Prediction of the thermal wake function due to M_k heating. (a) Prediction of Eq. (12) and (b) prediction of Eq. (13).

3.5. Verification of superposition technique

To verify the superposition technique used to predict a certain block temperature by Eq. (6) using Eqs. (7)–(14) in the case of multiple heating of all the blocks, a set of experiments were carried out with heating all the blocks at the same time and the measurement of the temperature rise of each block was conducted. Fig. 15 shows the temperatures of the blocks predicted by the superposition techniques superimposed on the same graph of the measured temperatures of the blocks in the case of multiple heating of the blocks for $Re = 1500$ and $H/B = 5$ as a sample of results. The figure shows that the superposition technique

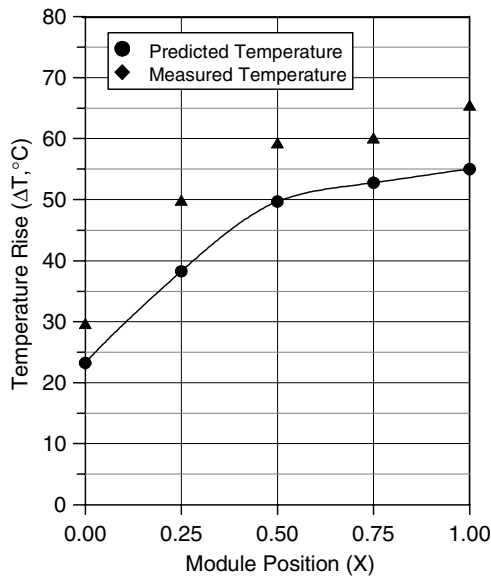


Fig. 15. Comparison between measured temperatures and those predicted by superposition technique.

under predicts the temperature rise of the blocks by 20%. This deviation can be attributed to the heat transfer by conduction, in a direction opposite to the direction of the spent flow, through the plate carrying the modules in the case of multiple heating. This conducted heat raises the temperature of the upstream blocks of each block. This heat was not included in the superposition technique.

3.6. Comparison with in-line array cooling

A numerical comparison between the proposed cooling techniques for the present study with in-line array cooling technique carried out by previous investigators is difficult due to the different in the geometric and flow parameters of the present work and previous works. However, a quantitative comparison between the proposed cooling technique of the present work with in-line cooling technique carried out by Anderson and Moffat [2] was conducted. Both techniques showed the increase of the adiabatic heat transfer coefficient of a module with the decrease of the module distance from the flow entrance, the increase of the air velocity over the module and the decrease of the channel height. Fig. 16 shows the comparison of the adiabatic heat transfer coefficient of the present work for the case of $H/B = 3$ with that obtained by Anderson and Moffat [2] for in-line array cooling at $H/B = 2.25$. The spent air flow velocity of the present work corresponding to the studied range of Re (500–2500) is in the range (0.14–0.7 m/s). Fig. 16 shows that the adiabatic heat transfer coefficient of the present work for $Re = 2500$ which is corresponding to spent air velocity of 0.7 m/s is slightly higher than that obtained by Anderson and Moffat [2] for in-line cooling at 3 m/s air velocity. This means that for the same air flow velocity over the module one can predict from Fig. 16 that the adiabatic heat transfer coefficient for the

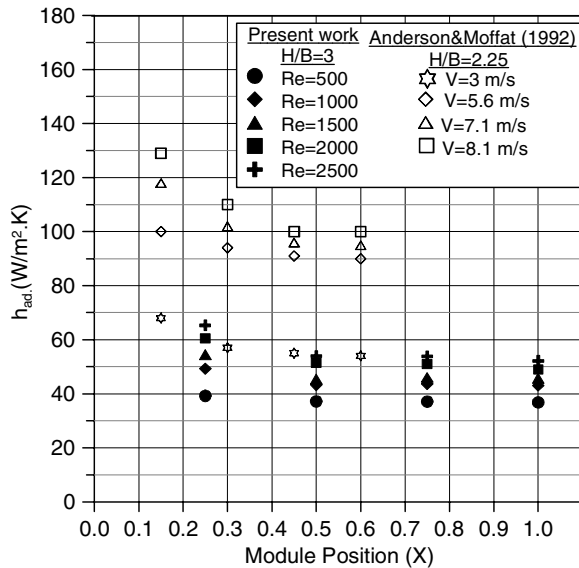


Fig. 16. Comparison of the present results with the previous work.

proposed cooling techniques is very high compared to those of in line array cooling.

4. Conclusions

An experimental study of cooling an array of multiple heat sources simulating electronic equipment by a single row of slot air jets positioned above a critical row was conducted. The heat transfer rates from the critical blocks just below the slot air jets and from the other blocks away from the jets were studied. The effects of air Reynolds number, the position of the heated block and the clearance distance between the heated blocks and the plate from which the jets was discharged on the Nusselt number were investigated. The results showed that the Nusselt number at the stagnation point was maximum at a certain H/B and increases with the increase of Re . The Nusselt number of the blocks away from the jet increased with both of the decrease of its distance from the jet, the increase of air Reynolds number and the decrease of H/B . Correlations of the adiabatic Nusselt number in terms of the parameters X , Re and H/B were presented.

The thermal wake effect of each heated block on the down stream blocks was studied and correlated in terms of the parameters Re and H/B . The superposition technique with the correlations of the Nusselt number and the thermal wake functions was used to predict the operating temperature of any block of the array in the case of multiple heating. More experimental runs were carried out with applying power to all the blocks at the same time in order to measure the thermal wake effect and comparing it with the predicted one using the superposition technique. It was found that the superposition technique under predicts the temperatures of heated blocks in the case of multiple heating.

References

- [1] A.M. Anderson, R.J. Moffat, Direct air cooling of electronic components: reducing component temperature by controlled thermal mixing, *International Journal of Heat Transfer* 113 (1991) 56–62.
- [2] A.M. Anderson, R.J. Moffat, The adiabatic heat transfer coefficient and the superposition kernel function: Part1 – Data for arrays of flat packs for different flow conditions, *International Journal of Electronic Packaging* 114 (1992) 14–21.
- [3] D.E. Arvizu, R.J. Moffat, The use of superposition in calculating cooling requirements for circuit board mounted electronic components, in: *Proceedings of the 32nd Electronic Components*, IEEE 32 (1982) 133–144.
- [4] K. Azar, R.J. Moffat, Evaluation of different heat transfer coefficient definitions, *Journal of Electronic Cooling* 1 (1995) 21–23.
- [5] R.J. Moffat, D.E. Arvizu, A. Ortega, Cooling electronic components: forced convection experiments with an air cooled array, heat transfer in electronic equipment, *ASME HTD* 48 (1985) 17–27.
- [6] R.J. Moffat, A.M. Anderson, Applying heat transfer coefficient data to electronic cooling, *Journal of Heat Transfer* 112 (1990) 882–890.
- [7] E.M. Sparrow, J.E. Niethammer, A. Chaboki, Heat transfer and pressure drop characteristics of arrays of rectangular modules encountered in electronic equipment, *International Journal of Heat and Mass Transfer* 25 (1982) 961–973.
- [8] E.M. Sparrow, S.B. Vemuri, D.S. Kadle, Enhancement and local heat transfer, pressure drop and flow visualization for array of blocks-like electronic equipment, *International Journal of Heat and Mass Transfer* 26 (1983) 689–699.
- [9] R.A. Wirtz, P. Dykshoorn, Heat transfer from arrays of flat packs in a channel flow, in: *Proceedings of the Fourth Annual International Electronic Packaging Society*, Baltimore MD, 1984, pp. 247–256.
- [10] M. Molki, M. Faghri, O. Ozbay, A correlation for heat transfer and wake effect in the entrance region of an in-line array of rectangular blocks simulating electronic components, *International Journal of Heat Transfer* 117 (1995) 40–46.
- [11] B.A. Jubran, S.A. Swity, M.A. Hamdan, Convection heat transfer and pressure drop characteristics of various array configurations to simulate the cooling of electronic modules, *International Journal of Heat and Mass Transfer* 39 (1996) 3519–3529.
- [12] R.J. Yang, L.M. Fu, Thermal and flow analysis of heated electronic components, *International Journal of Heat and Mass Transfer* 44 (2001) 2261–2275.
- [13] G.K. Morris, S.V. Garmella, Thermal wake downstream of a three-dimensional obstacle, *Experimental Thermal and Fluid Science* 12 (1996) 65–74.
- [14] G.K. Morris, S.V. Garmella, Composite correlation for convection heat transfer from arrays of three dimensional obstacles, *International Journal of Heat and Mass Transfer* 40 (1997) 493–498.
- [15] G. Recktenwald, Use of Superposition to Describe Heat Transfer from Multiple Electronic Components, CFD Report, Mechanical Engineering Department, Portland State University, Portland, Oregon, 2001.
- [16] E. Baydar, Confined impinging air jet at low Reynolds numbers, *Experimental Thermal and Fluid Science* 19 (1999) 27–33.
- [17] L.A. Brignoni, S.V. Carmella, Effect of nozzle-inlet chamfering on pressure drop and heat transfer in confined air jet impingement, *International Journal of Heat and Mass Transfer* 43 (2000) 1133–1139.
- [18] D.W. Colucci, R. Viskanta, Experimental measurements of the flow and heat transfer of a square jet impinging on an array of square pin fin, *Experimental Thermal and Fluid Science* 13 (1996) 71–80.
- [19] G. Robert, J.C. Akfirat, Heat transfer characteristics of impinging two-dimensional air jets, *International Journal of Heat Transfer* (1966) 101–108.
- [20] S.V. Garmella, R.A. Rica, Confined and submerged liquid jet impingement heat transfer, *International Journal of Heat Transfer* 117 (1995) 871–877.

- [21] R.J. Goldstein, K.A. Sobolik, W.S. Seol, Effect of entrainment on the heat transfer to a heated circular air jet impinging on a flat surface, *International Journal of Heat Transfer* 112 (1990) 608–611.
- [22] J.P. Hartnett, T.F. Irvine, Heat and mass transfer between impinging gas jets and solid surfaces, *Advances in Heat Transfer* 13 (1977) 1–60.
- [23] H. Lianmin, M.S. El-Genk, Heat transfer of an impinging jet on a flat surface, *International Journal of Heat and Mass Transfer* 37 (1993) 1915–1923.
- [24] D.H. Lee, Y.M. Lee, Y.T. Kim, S.Y. Won, Y.S. Chung, Heat transfer enhancement by the perforated plate installed between an impinging jet and the target plate, *International Journal of Heat and Mass Transfer* 45 (2002) 213–217.
- [25] Z.H. Lin, Y.J. Chou, Y.H. Hung, Heat transfer behaviors of confined slot jet impingement, *International Journal of Heat and Mass Transfer* 35 (1996) 1097–1107.
- [26] A.K. Mohanty, A.A. Tawfek, Heat transfer due to round jet impinging normal to a flat surface, *International Journal of Heat and Mass Transfer* 37 (1992) 1639–1647.
- [27] A.R.P. Van-Heiningen, A.S. Mujumdar, W.J.M. Douglas, Numerical prediction of the flow field and impingement heat transfer caused by a laminar slot jet, *International Journal of Heat Transfer* 98 (1976) 654–658.
- [28] D.C. Wadsworth, I. Mudawar, Cooling of a multichip electronic module by mean of confined two-dimensional jets of dielectric liquid, *International Journal of Heat Transfer* 112 (1990) 891–898.
- [29] B.R. Hollworth, M. Durbin, Impingement cooling of electronics, *International Journal of Heat Transfer* 114 (1992) 607–613.
- [30] N.V. Suryanarayana, *Engineering Heat Transfer*, West Publishing Company, New York, 1995.
- [31] J.P. Holman, W.J. Gajda, *Experimental Methods for Engineers*, McGraw Hill, New York, 1989.
- [32] A. Faris, *Slot Jet Impingement Air Cooling of Multiple Heat Sources*, M.Sc. thesis, Benha High Institute of Technology, Benha, Egypt, 2004.
- [33] S.J. Kim, S.W. Lee, *Air Cooling Technology of Electronic Equipment*, CRC Press, Inc., New York, 1996.